Why Is the Spreading of the North Pacific Intermediate Water Confined on Density Surfaces around $\sigma_\theta = 26.8$?*

BO QIU

Department of Oceanography, University of Hawaii at Manoa, Honolulu, Hawaii

1 October 1993 and 3 May 1994

ABSTRACT

The North Pacific Intermediate Water, characterized by a salinity minimum confined to density surfaces of $\sigma_\theta = 26.7$–26.9, exists throughout the subtropical gyre and has been observed to originate in the subarctic North Pacific. The physical processes that determine the density range on which the NPIW resides are not yet well understood. This study attempts to clarify these processes by combining observational data and a simple advection–diffusion isopycnal model. Due to the regional excessive precipitation over evaporation, the salinity in the upper-layer subarctic North Pacific generally decreases with decreasing water depth. Both alongisopycnal advection and diffusion work to carry this salinity/depth characteristic into the subtropical circulation. For the isopycnal surfaces overlying the NPIW, however, this transport mechanism is hindered by the seasonal outcropping. The outcropping not only blocks the fresh subarctic water from advecting and diffusing along these isopycnals into the subtropical gyre, but also results in shoaling of the isopycnals in the Kuroshio–Oyashio mixed water region, where the turbulent mixing in the deep winter mixed layer is able to conduit the surface salt flux into these outcropping isopycnal surfaces. This seasonal forcing creates a high-salinity overlying layer, leaving $\sigma_\theta = 26.7$–26.9 the lightest density surfaces that are free to transport the uppermost (i.e., the freshest) subarctic water into the subtropical North Pacific. This model result is consistent with high-resolution CTD observations that showed that $\sigma_\theta = 26.7$–26.9 are the least dense isopycnal surfaces on which the alongisopycnal potential vorticity is homogenized. The NPIW surfaces contrast with the shallower isopycnal surfaces where strong potential vorticity gradients exist.

1. Introduction

A prominent feature of the subtropical North Pacific Ocean that differs from its counterpart in the North Atlantic Ocean is the presence of a relatively low salinity tongue of water intruding from the northern subarctic region. This salinity minimum water, dubbed by Sverdrup et al. (1942) as the North Pacific Intermediate Water (NPIW), is found in almost the entire subtropical gyre, and many previous studies have shown that its existence is confined within a relatively narrow density range centered at $\sigma_\theta = 26.8$ (e.g., Reid 1965; Hasunuma 1978; Talley 1993). The formation of the NPIW is different from that of the shallow salinity minimum, whose existence in the eastern North Pacific has been successfully explained by Talley (1985) using the wind-driven ventilated thermocline theory (Luyten et al. 1983). Because the 26.8 σ_θ surface does not outcrop in the North Pacific Ocean (with the exception of the Okhotsk Sea: Talley 1991) and because the wind stress curl over the subarctic North Pacific is mostly positive (e.g., Hellerman and Rosenstein 1983), mechanisms other than the direct, wind-driven ventilation are required to account for the formation of the NPIW.

To explain the formation of the NPIW, Reid (1965) hypothesized that the vertical mixing in the subarctic gyre transfers fresh, cold, and oxygen-rich surface water through isopycnals and that the lateral mixing and advection are responsible for the spreading of the NPIW in the subtropics. Based on the distribution of water characteristics in the Oyashio–Kuroshio mixed water region (west of 155°E and north of 30°N), Hasunuma (1978) speculated that the NPIW is not a distinct water mass but a result of the warm, saline Kuroshio water overrunning the less saline Oyashio water.

As suggested by Reid (1965), understanding the NPIW involves two fundamental questions. The first question is what physical processes are responsible for conduiting the fresh, subarctic surface water downward to the NPIW density levels. The only source of freshwater in the North Pacific exists in the surface subarctic region due to the regional excessive precipitation over evaporation. Rather than a sharp halocline forming near the sea surface, however, the observed salinity profiles in the subarctic North Pacific indicate that the salinity gradually increases with depth. The details of

* SOEST Contribution Number 3631.

Corresponding author address: Dr. Bo Qiu, Dept. of Oceanography, School of Ocean and Earth Science and Technology, University of Hawaii at Manoa, 1000 Pope Road, Honolulu, HI 96822.

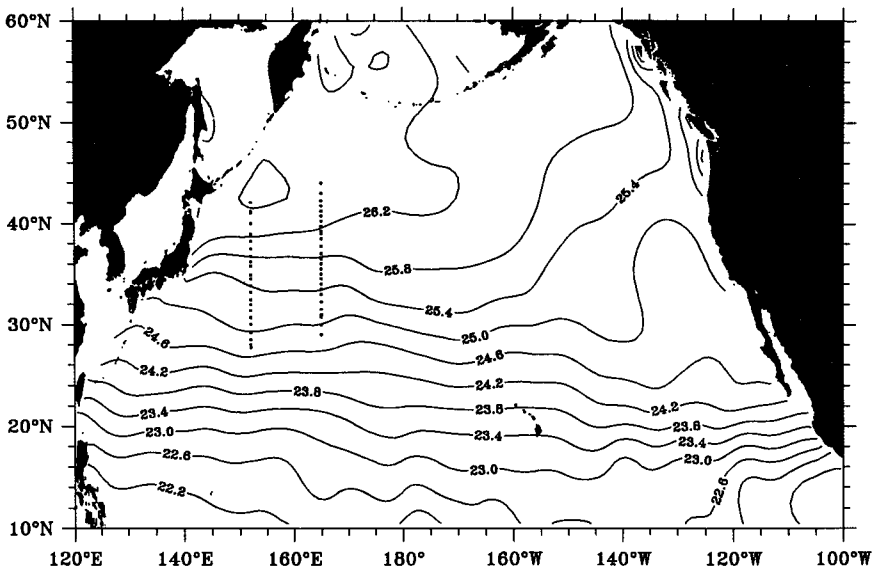

FIG. 1. Sea surface density from the Levitus (1982) March climatological dataset. Solid dots along 152° and 165°E indicate the surface-to-bottom CTD stations. The observed results are shown in Figs. 2–4.

the vertical mixing process in the western subarctic gyre have recently been explored by Talley (1991): she showed that the freshening and oxygenation at the 26.8 σ_θ surface can occur in the Okhotsk Sea through brine rejection below the ice formation. Van Scoy et al. (1991), on the other hand, stressed the role played by the Alaskan Gyre, where negative buoyancy fluxes and wind stirring caused by severe winter conditions enhance vertical turbulent mixing and transmit less saline surface water to the NPIW density levels.

The second relevant question is why the NPIW, which exists exclusively in the subtropical gyre as a salinity minimum, preferentially resides on the isopycnal surfaces of σ_θ = 26.7–26.9. In the subarctic North Pacific, the salinity increases monotonically with water depth. Since the fresher water exists in the shallower subarctic layer, it is not obvious why the spreading of the low-salinity water into the subtropical gyre should be confined to this particular density range. So far, the question of what sets the density level at which the NPIW spreading occurs has not been satisfactorily answered. The present study attempts to answer this question from analyses of CTD data and from diagnostic calculations using an advection–diffusion isopycnal model. It is shown that the NPIW density is preferentially selected around σ_θ = 26.8 because the overlying isopycnals outcrop in the Kuroshio–Oyashio mixed water region in winter. This outcropping blocks the fresh subarctic water from advecting and diffusing along these isopycnals into the subtropical gyre. It also causes shoaling of these isopycnals so that they are under the direct influence of the turbulent mixing of the surface mixed layer. Since the winter evaporation rate exceeds the precipitation rate in the Kuroshio–Oyashio mixed water region, the contact with the mixed layer conduits the surface salt flux onto the outcropping isopycnal surfaces. It is emphasized that because σ_θ = 26.7–26.9 are the *lightest* density surfaces that do not undergo this seasonal change, a low-salinity tongue of water is free to penetrate into the subtropical circulation, thus creating a local salinity minimum (the NPIW) in this particular density range.

2. Meridional features across the North Pacific subtropical–subarctic gyres

We start by investigating some of the observed meridional features across the subtropical–subarctic gyres in the western North Pacific Ocean. Comprehensive descriptions of this part of the ocean have been given by many previous authors (Reid 1965; Masuzawa 1972; Kawai 1972; Talley 1993; among others). The investigation here complements those studies and focuses on aspects relevant to later discussions.

During the early 1980s, seven repeated hydrographic–CTD surveys across the Kuroshio–Oyashio current system in the western North Pacific were conducted by the CTD groups at Scripps Institute of Oceanography and Woods Hole Oceanographic Institution (Fig. 1). These surveys provided the first surface to bottom, high-resolution CTD sections across the Kuroshio–Oyashio; Niiler et al. (1985), Joyce (1987), and Joyce and Schmitz (1988) have summarized many scientific results from these cruises. Results from three of these cruises are presented in this study (Table 1). These three cruises are chosen because they reach far

TABLE 1. Summary of the CTD cruises. All data were collected from the R/V *T. Thompson*.

Section	Dates (d/mo/yr)	Station number	Figure
152°E	25/5/82–5/6/82	3–26	2
165°E	9/9/84–8/10/84	3–29	3
165°E	25/11/83–4/12/83	10–28	4

enough north to cover the Oyashio Front (also known as the Subarctic Front) and represent the oceanic conditions in different seasons. (Similar meridional structures were obtained from the other four cruises and are not presented here for conciseness.) Figures 2–4 show the meridional sections of (a) potential density σ_θ, (b) salinity S, and (c) potential vorticity Q from the three cruises. Following Hall and Fofonoff (1993), the potential vorticity here is defined as

$$Q = -\frac{1}{\rho_0}\left[\left(f - \frac{\partial u}{\partial y}\right)\frac{\partial \sigma_\theta}{\partial z} + \frac{\partial u}{\partial z}\frac{\partial \sigma_\theta}{\partial y}\right], \qquad (1)$$

where f is the Coriolis parameter, ρ_0 is the reference density, and u is the zonal velocity component calculated geostropically relative to 2000-db depth. This depth was suggested by Roemmich and McCallister (1989) to be an appropriate reference level for the subtropical–subarctic North Pacific Ocean.

During these CTD surveys, the axis of the Kuroshio Extension exists at 33°N in Fig. 2a and at 34.5°N in Figs. 3a and 4a. The Oyashio Front is located in all cases around 41.5°N, although the existence of a warm-core ring in the 1984 cruise (Fig. 3a) makes the distinction between the Oyashio Front and the northern flank of the warm core ring ambiguous. Seasonal differences among the three cruises are obvious in the surface layer. During the May–June cruise when surface warming takes place (Fig. 2), the seasonal thermocline is in the developing stage. To the south of the Kuroshio Extension, it overrides a thick layer of low potential vorticity, commonly known as the subtropical mode water (STMW; Masuzawa 1969). The seasonal thermocline is fully developed during September–October (Fig. 3), and the size of the STMW (the low potential vorticity area) along this 165°E section is relatively small as compared to the 152°E section of Fig. 2. The lesser STMW found in Fig. 3 could be due to the diffusive effect from the progression of the seasonal thermocline, and it could also be a result of geographic differences. [The source region of the STMW is between 140° and 155°E where winter surface cooling is strongest; see Hanawa (1987).] As in Fig. 2, the cruise shown in Fig. 3 also captured a cutoff warm core ring; it is evident from the S and Q sections that these warm core eddies are effective in transporting higher salinity and lower potential vorticity Kuroshio Extension water into the Kuroshio–Oyashio mixed water region. Since the surface thermal forcing in this region changes to the cooling phase around the autumnal equinox, Fig. 4 reveals that the seasonal thermocline formed in summer is being replaced by the new winter mixed layer in November–December. [For a thorough discussion of the upper-ocean heat balance in the Kuroshio Extension region, readers are referred to Qiu and Kelly (1993).]

Despite these differences due to seasonal changes and mesoscale oceanic fluctuations, several features exist in common to the three cruises. For example, the

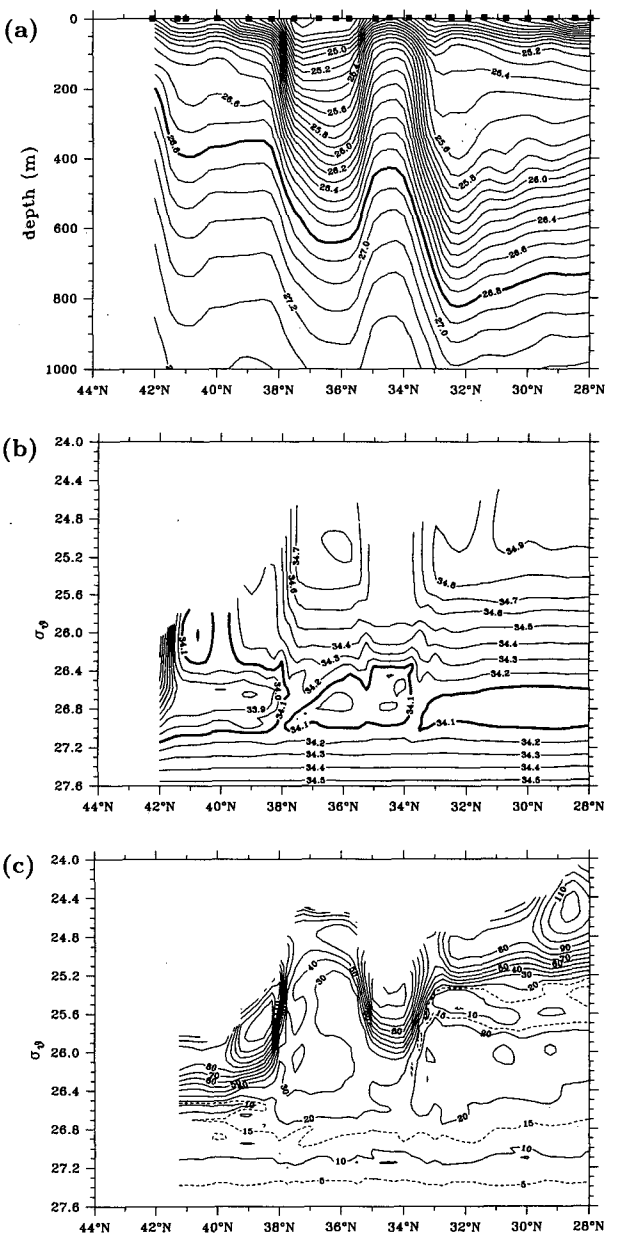

FIG. 2. Meridional sections from the 1982 CTD cruise along 152°E (see Table 1). Solid dots in (a) indicate the location of CTD stations. (a) Water density vs depth, (b) salinity vs density, and (c) potential vorticity vs density (units are 10^{-11} m^{-1} s^{-1}).

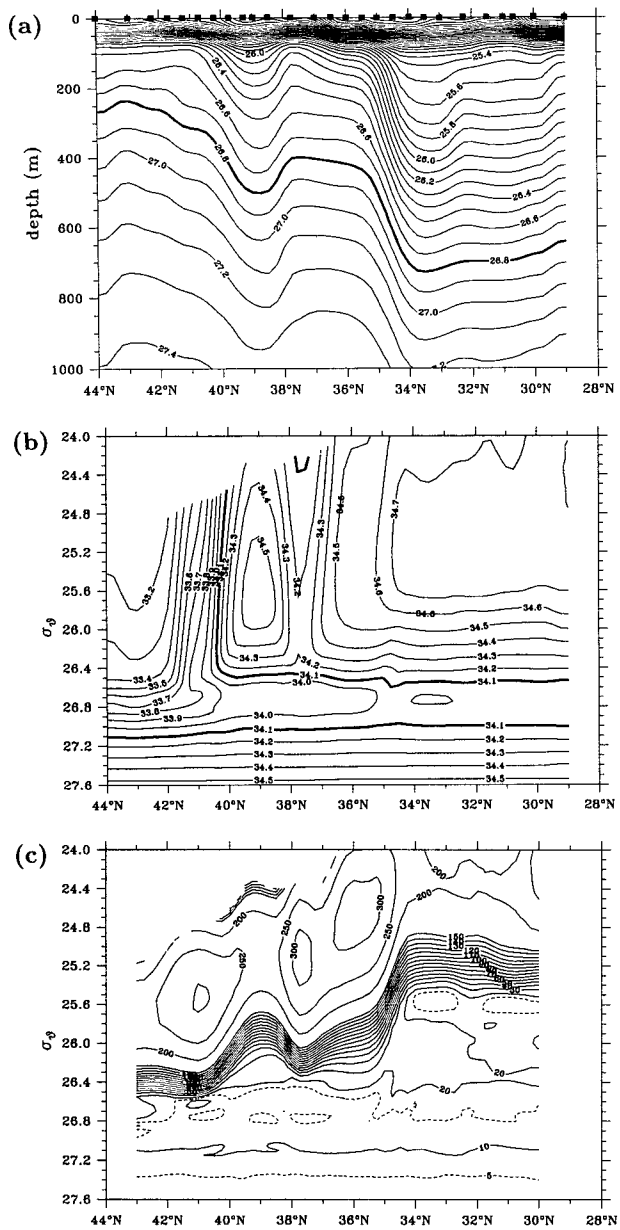

FIG. 3. Same as Fig. 2 except for the 1984 CTD cruise along 165°E (see Table 1).

Oyashio Front near 41°–42°N is always accompanied by a sharp salinity gradient. All cruises indicate that intrusion of the low salinity water occurs below the seasonal thermocline in the Oyashio Front region (i.e., below the 26.6σ_θ surface). Although strong eddy motions of the warm core rings and the Kuroshio Extension may intermittently distort the alongisopycnal intrusions (e.g., Fig. 2b), the presence of the low salinity tongue between the $\sigma_\theta = 26.6 \sim 27.0$ surfaces is stable. As noticed by many previous investigators, the core of the salinity minimum resides on the isopycnal surface of $\sigma_\theta = 26.8$.

Another common feature in Figs. 2–4 is that, separated by the 26.6 σ_θ surface, the alongisopycnal potential vorticities transit from an upper layer with prominent horizontal gradients to a lower layer where Q is mostly uniform. Similar potential vorticity structures can be discerned in the Q maps computed from the Levitus (1982) climatology dataset (Talley 1988). In light of the theories of Luyten et al. (1983) and Rhines and Young (1982), the transition in the potential vorticity structure per se is not surprising. The 26.6 σ_θ surface, as shown in Fig. 1, is essentially the

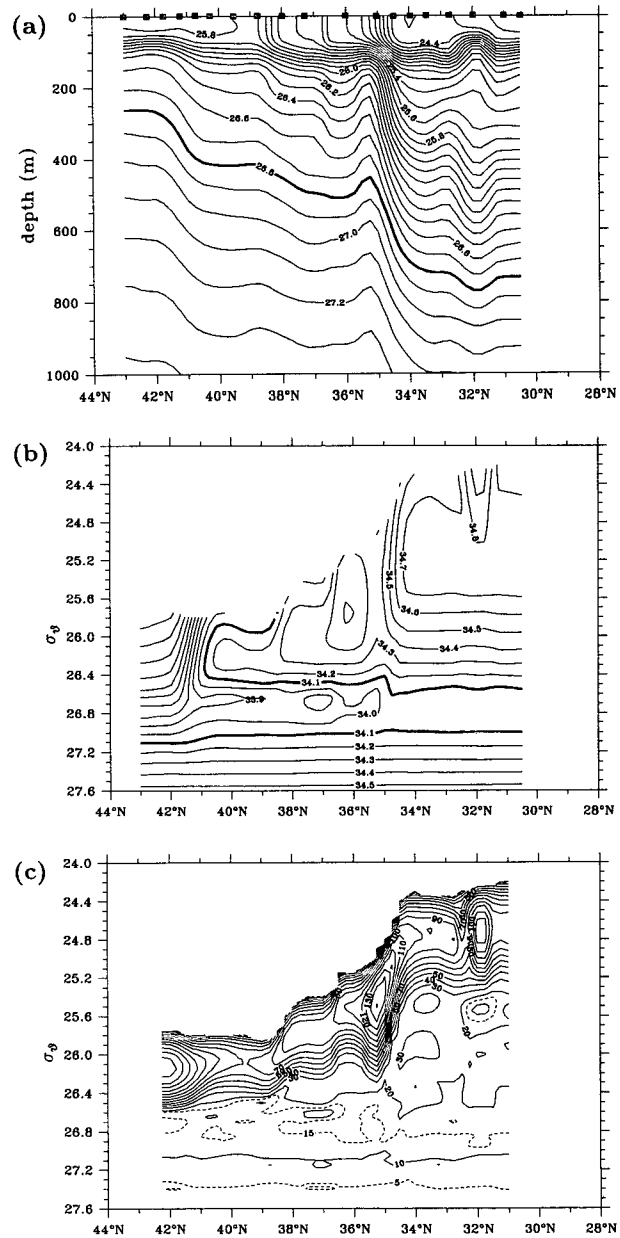

FIG. 4. Same as Fig. 2 except for the 1983 CTD cruise along 165°E (see Table 1).

densest isopycnal surface outcropping in winter in the North Pacific; layers above this isopycnal surface are directly ventilated and their potential vorticities are determined by spatially and temporally fluctuating surface wind and buoyancy forcings. As predicted by the Rhines and Young theory, in the unventilated layers below $\sigma_\theta = 26.6$, a homogenized Q region is likely to exist due to repeated motions along closed geostrophic contours. What is unclear is how the coexistence of the ventilated and unventilated layers will influence the intrusion of the low salinity tongue (NPIW) in the subtropical North Pacific. This question is addressed in the following sections.

3. Isopycnal intrusion of the low-salinity tongue

From the CTD sections shown in Figs. 2–4, it is clear that the salinity minimum water of NPIW originates in the Oyashio Front north of the Kuroshio–Oyashio mixed water region. Since the source of the freshwater in the subarctic North Pacific is the year-round, regional negative $E - P$ flux (see Fig. 11 in the next section), the fact that the observed salinity in the subarctic region increases rather smoothly with depth (in Figs. 2–4) suggests the importance of the vertical mixing processes in determining the salinity profiles there. Although understanding the vertical mixing processes is itself an important issue, this is not pursued in the present study. In the following discussion, we will assume that the source of low-salinity water exists in the subarctic gyre (i.e., the salinity profiles along 42°N will be specified from observations) and focus on the intrusion of the low-salinity tongue into the subtropical North Pacific using a simple model.

a. *Advection–diffusion model*

Given a conservative property such as salinity, the equation governing its alongisopycnal changes is

$$\frac{\partial S}{\partial t} + \frac{1}{a\cos\phi}\frac{\partial}{\partial \lambda}(uS) + \frac{1}{a\cos\phi}\frac{\partial}{\partial \phi}(vS\cos\phi) = A_i\left[\frac{1}{a^2\cos^2\phi}\frac{\partial^2 S}{\partial \lambda^2} + \frac{1}{a^2\cos\phi}\frac{\partial}{\partial\phi}\left(\frac{\partial S}{\partial \phi}\cos\phi\right)\right] + \frac{\partial}{\partial z}\left(A_d\frac{\partial S}{\partial z}\right), \quad (2)$$

where a is the radius of the earth, ϕ is latitude, λ is longitude, u and v are the eastward and northward components of velocity, and A_i and A_d are coefficients of isopycnal and diapycnal eddy diffusions for the salinity. With the focus on the subtropical gyre of the North Pacific, the model domain in the present study is chosen from 14° to 42°N and 120°E to 120°W. This domain, as indicated by Talley (1993, her Fig. 3), covers the entire area of the observed NPIW, except in regions off Vancouver where part of the NPIW extends into the subarctic gyre and along the Mindanao coast where part of the NPIW is carried southward by the Mindanao Current (Bingham and Lukas 1994).

To simplify the model physics, we will neglect below the diapycnal mixing term in Eq. (2). This simplification makes it possible to determine independently the salinity distributions among different isopycnal surfaces. Possible effects of the diapycnal mixing on the model results, however, will be discussed in section 4. Along the model's open boundaries, salinity values are fixed using the Levitus (1982) climatology. Like the rationale mentioned above for the model's northern boundary along 42°N, high salinity waters along the model's southern and eastern walls have their origins in the South Pacific Ocean, and it is beyond the scope of this study to directly determine the salinity values in the tropical circulation. Along the model's "closed" boundaries, namely, boundaries where water depths are shallower than 1000 m, the no-lateral-flux condition is imposed.

To estimate the (u, v) components of velocity on the isopycnal surfaces, we compute the acceleration potentials relative to 2000-m depth from the Levitus dataset. Choosing the reference level at 2000-m depth again follows the study by Roemmich and McCallister (1989). As an example, Fig. 5 shows the acceleration potential (A) values on the 26.8 σ_θ surface, and they are related to the alongisopycnal velocities by

$$-2\Omega\sin\phi v = -\frac{1}{a\cos\phi}\frac{\partial A}{\partial \lambda}, \quad (3)$$

$$2\Omega\sin\phi u = -\frac{1}{a}\frac{\partial A}{\partial \phi}, \quad (4)$$

where Ω is the rotation rate of the earth. Strictly speaking, Eqs. (3)–(4) give u, v on steric anomaly surfaces. To estimate u, v on the isopycnal surfaces, a correction term is required (Cochrane et al. 1979). This correction term is not included because its effect is small compared with the velocity errors introduced by the uncertainty in the choice of the reference level.

Given the boundary values and the velocity field, the salinity distribution on an isopycnal surface can be determined numerically. By defining S and A, respectively, at the center and corners of 1° × 1° box, we integrated the finite-difference forms of Eqs. (2)–(4) until the salinity field reached the steady state. In the calculation, $A_i = 1500\ \text{m}^2\ \text{s}^{-1}$ is used. This value follows Jenkins (1991) who, from tritium–helium observations, estimated the isopycnal eddy diffusivity in the main thermocline of the Sargasso Sea to be 1840 $\pm$ 440 $\text{m}^2\ \text{s}^{-1}$. Choosing other A_i values in the range of 1000–2000 $\text{m}^2\ \text{s}^{-1}$ produces qualitatively similar results to be presented below. For simplicity in discussion, we will focus on the model results from three isopycnal surfaces: 1) $\sigma_\theta = 26.8$, on which the NPIW core resides, 2) $\sigma_\theta = 27.0$, which represents the isopycnal surfaces

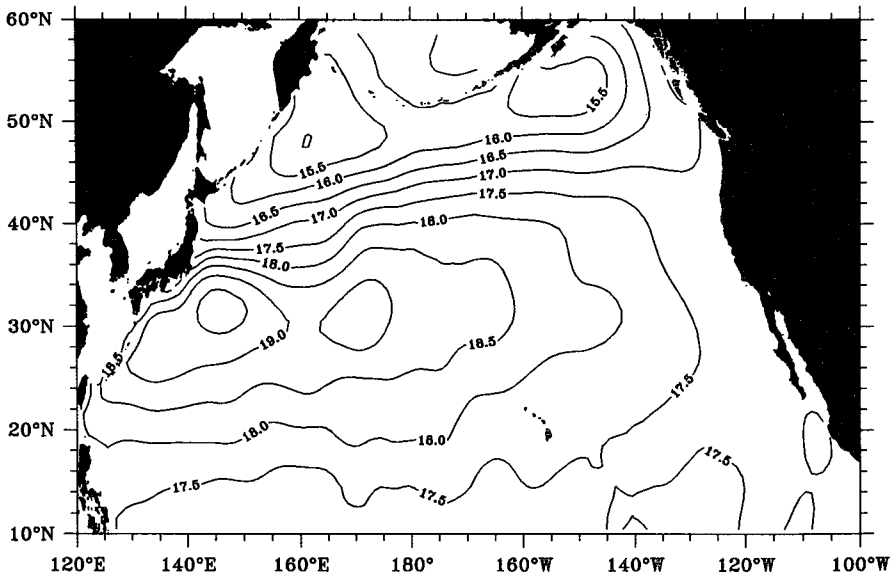

FIG. 5. Acceleration potential on the 26.8 σ_θ surface relative to 2000-m depth. Contours have units $m^2\ s^{-2}$ and are calculated from the annual Levitus climatology.

below the NPIW core, and 3) σ_θ = 26.2, which represents the isopycnal surfaces above.

b. *Modeled salinity distribution on the NPIW core surface*

Figure 6b shows the salinity distribution on the σ_θ = 26.8 isopycnal surface from the model calculation. Comparing it with the Levitus climatology (Fig. 6a) reveals that the observed and the modeled salinity patterns are generally similar. The noted discrepancies occur along the western boundary and in the Kuroshio Extension's recirculation region. The modeled salinity along the western boundary from Taiwan to the Japan coast, for example, is not as high as from the observations. In the recirculation region of the Kuroshio Extension (140°–170°E, 30°–35°N), observations indicate a well-developed, C-shaped salinity pattern (see the 34.1 psu contour), but this pattern is not as clear in the model result. A possible reason for these discrepancies is the uncertainty in the velocity field. Choosing the no-motion level at 2000-m depth along the western boundary may well underestimate the intensity of the Kuroshio, resulting in a smaller northward salt flux. Similarly, the assumption of a level of no motion misses the barotropic component of the Kuroshio Extension recirculation gyre (see Joyce and Schmitz 1988) and consequently weakens the anticyclonic intrusion of the low salinity water to the south of the Kuroshio Extension. Despite these problems, the generally good agreement between Figs. 6a and 6b suggests that the alongisopycnal advection–diffusion is the essential mechanism for the low-salinity water intrusion on the NPIW core surface.

c. *Modeled salinity distribution below the NPIW core*

Like for the σ_θ = 26.8 isopycnal surface, the model results for isopycnal surfaces below the NPIW core also agree well with the observations. For example, Fig. 7b shows the modeled salinity distribution on the σ_θ = 27.0 isopycnal surface. It compares favorably with the observed salinity pattern (Fig. 7a), except again in the recirculation region of the Kuroshio Extension where the modeled anticyclonic intrusion of the fresh, subarctic-origin water is weak compared with the observations.

d. *Modeled salinity distribution above the NPIW core*

Figure 8b shows the modeled salinity distribution on the σ_θ = 26.2 surface, representative of the isopycnal surfaces above the NPIW core. Unlike the results presented above, the modeled salinity distribution deviates significantly from the observations (Fig. 8a). In a large portion of the model's interior, the modeled salinity values are 0.2–0.3 psu lower than the climatological data; these values are actually even lower than those on the NPIW core surface (Fig. 6b), implying that no salinity minimum is realized from the model calculation. Given that the shallower subarctic gyre in the North Pacific is fresher and that the salinity has little depth dependency along the model's southern boundary (compare Fig. 6a with Fig. 8a), the lower salinity in Fig. 8b is expected under the present assumed model dynamics. In fact, the water along the North American continent is observed to be fresher on the σ_θ = 26.2 surface than on σ_θ = 26.8, and this is simulated in the

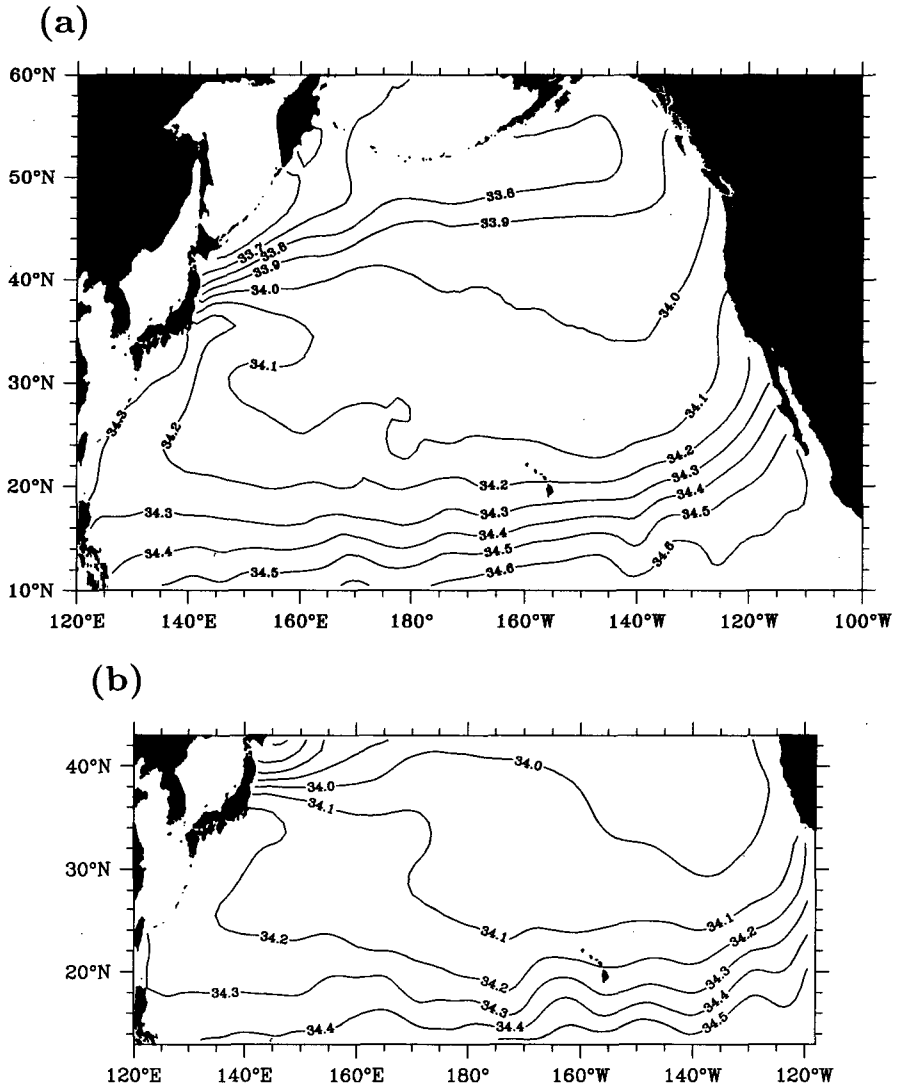

FIG. 6. (a) Salinity distribution on the 26.8 σ_θ surface from the Levitus climatology. (b) Modeled salinity distribution on this same density surface. The model is governed by Eq. (2), and the salinity values along the model's open boundaries are fixed by the Levitus annual climatological data.

model. But, clearly, the present model lacks the dynamics that create a saltier upper layer west of the offshore region of the North American continent. In the next section, we will try to clarify the underlying dynamics for the saltier upper layer. As shown below, this in turn helps us understand why the salinity minimum core exists on the σ_θ = 26.8 isopycnal surface.

4. Importance of the seasonal change for the layer above the NPIW core

In determining the alongisopycnal salinity distributions above, we relied on the Levitus climatological data to specify both alongisopycnal velocities and boundary salinity values. While the isopycnal surfaces above the NPIW core, such as σ_θ = 26.2, extend throughout the subarctic North Pacific in the annually averaged density field, they commonly outcrop in winter in the western North Pacific where the ocean is usually freshest (Figs. 1 and 8a). When an isopycnal surface outcrops, the alongisopycnal advective–diffusive processes no longer transport the fresh subarctic water into the subtropical circulation. Southward freshwater flux in this case occurs only through the diapycnal mixing due to large-amplitude current fluctuations and cold core ring activities. In the tropical gyre, on the other hand, there always exists a high salinity water supply with little seasonal fluctuations. This seasonality clearly creates a situation in which the outcropping isopycnal surfaces receive less freshwater influx from the western subarctic gyre and remain saltier than if there were no seasonal outcrops.

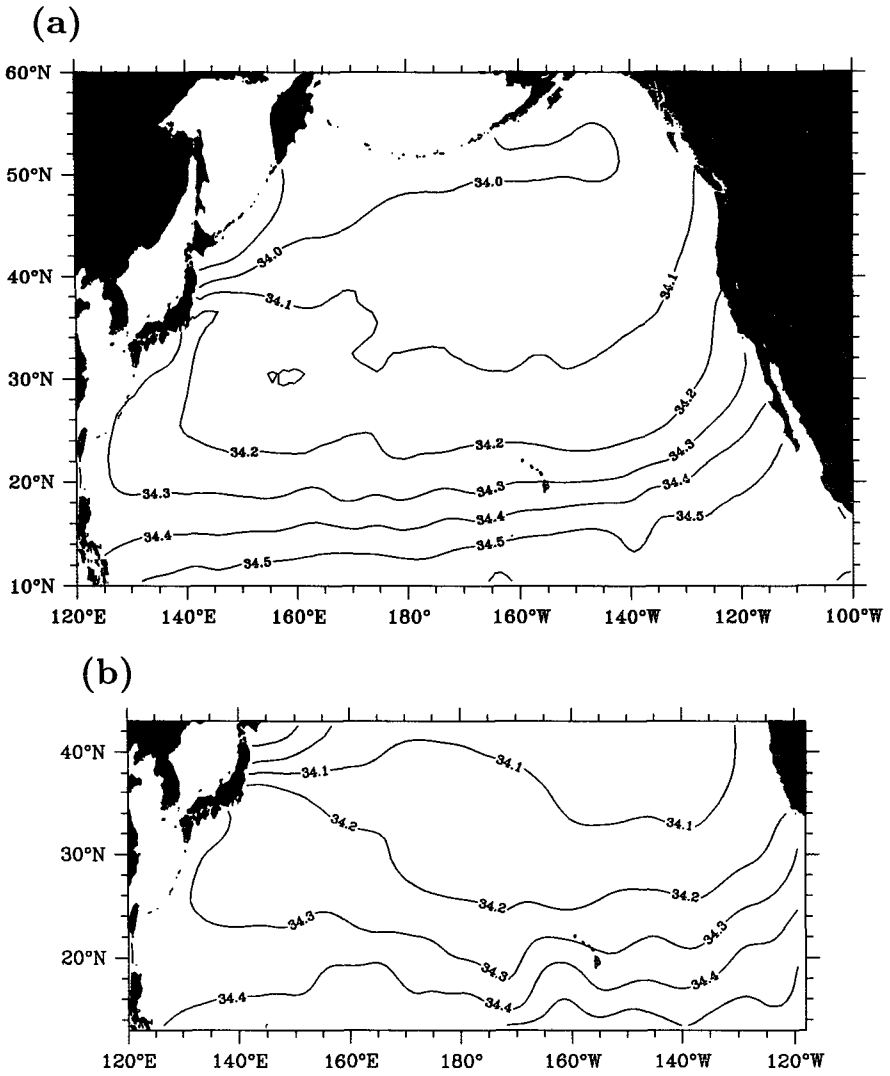

FIG. 7. Same as Fig. 6 except for the 27.0 σ_θ surface.

To quantitatively assess the importance of the isopycnal outcropping, we reformulate the model to allow for seasonal changes. From the seasonal Levitus dataset, we compute the acceleration potential fields for the four seasons and interpolate them linearly in time. Similarly, the salinity values along the model's boundaries are also linearly interpolated. When the isopycnal surface outcrops, we assume the salinity values along the outcropping line are equal to the seasonally varying climatological values. This boundary condition, rather than the nonflux condition $\partial S/\partial n = 0$ (where n is perpendicular to the outcropping line), is used because along the outcropping line the isopycnal surface is in direct contact with the atmosphere where surface salt fluxes exist due to local evaporation–precipitation. Figure 9 shows the salinity distribution on the $\sigma_\theta = 26.2$ surface obtained from this seasonally dependent model. The distribution is an annually averaged pattern after the model's seasonal pattern reached the steady state. Compared to the result without the seasonal change (Fig. 8b), the interior subtropical gyre is now saltier, a result expected from the above argument. The modeled salinity value in Fig. 9 is, however, still too fresh in comparison with the observations (by about 0.1 psu), suggesting that other physical processes should not be discounted.

One such physical process is the diapycnal mixing, which has been so far neglected in the model for simplicity. Diapycnal mixings can be particularly effective during the winter season in the Kuroshio Extension region. As shown by Talley (1984) and Hsiung (1985), the Kuroshio Extension is the region where the net heat flux from the ocean to the atmosphere is the largest in the entire North Pacific. Such a strong heat loss results in the deep winter mixed layer (~250 m in the Kuroshio Extension region: Hanawa and Hoshino

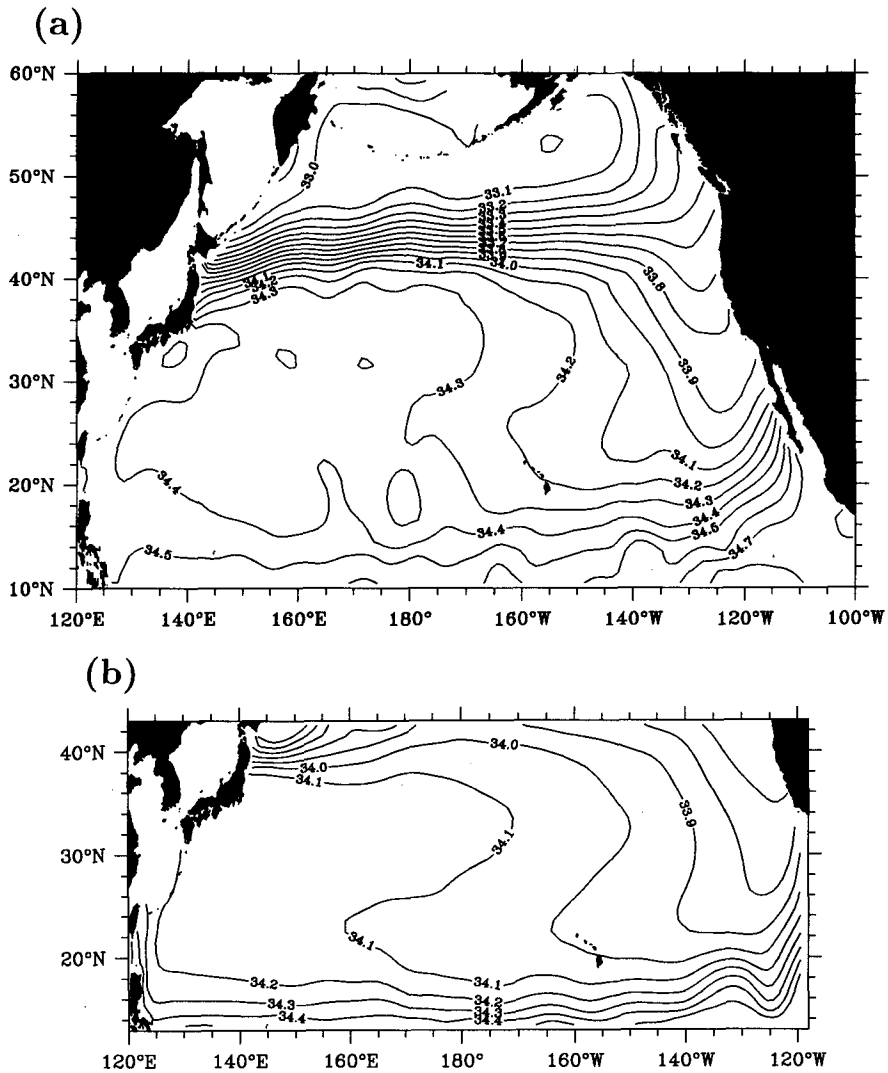

FIG. 8. Same as Fig. 6 except for the 26.2 σ_θ surface.

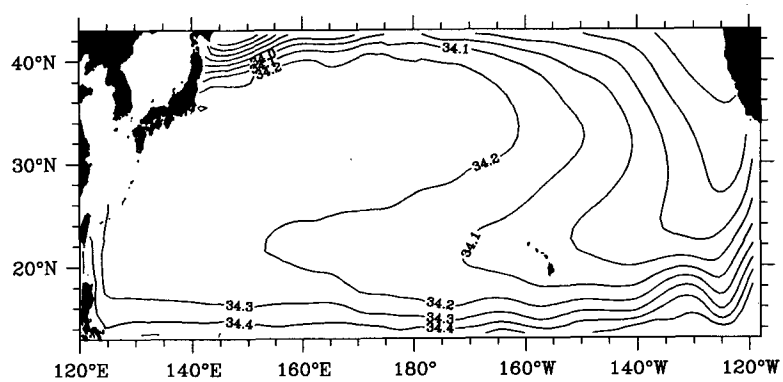

FIG. 9. Modeled salinity distribution on the 26.2 σ_θ surface including seasonal changes in the acceleration potential field and the salinity boundary values. Along the winter outcropping line, the salinity values are specified using the seasonally dependent climatological data.

1988; Qiu and Kelly 1993) and enhances diapycnal mixing in the upper ocean. Fully resolving this convective cooling process and its resultant diapycnal mixing, however, requires more sophisticated models than the one used here. Within the limits of the present model, a simple experiment is carried out to estimate the possible influence from diapycnal mixing. We assume that the diapycnal mixing is most effective in the region where the isopycnal depth is shallower than the mixed layer. For the case of the σ_θ = 26.2 surface in winter, for example, this assumption designates the region affected by diapycnal mixing to be where the isopycnal depth is shallower than 250 m in the Kuroshio Extension (see Fig. 10). Like along the outcropping line, we specify the salinity values in the "effective" region from the observations. The rationale for this is that when the isopycnal surface is shallower than the mixed layer, the enhanced turbulent mixing is likely to transfer the surface salt flux downward. Notice that the surface $E - P$ rate in the Kuroshio–Oyashio mixed water region is positive (evaporation exceeds precipitation) in fall/winter when the net surface heat flux is negative and the isopycnal outcropping takes place (see Fig. 11). Specifying the salinity values from the observations accounts for this downward salt flux in a diagnostic sense.

Figure 12 shows the salinity distribution obtained from the model under the above assumption. Despite the fact that the effective region is limited in space, extending only 200–300 km south of the outcropping line (Fig. 10), its influence upon the interior salinity content is significant. Compared to the result in Fig. 9, the salt influx from the mixed layer increases the salinity value in the central and western subtropical gyre by ~0.05 psu, which is now close to the climatological value shown in Fig. 8a. Discrepancies still exist between the modeled and the observed salinity distributions. The underestimated Kuroshio Current appears again to be responsible for the weak northward salt flux along the western boundary. Also, the criterion used above for defining the effective region by diapycnal mixing is subjective. Though small in magnitude, the diapycnal mixing in the interior of the subtropical gyre is likely to also influence the detailed salinity pattern on the σ_θ = 26.2 isopycnal surface. In spite of these uncertainties, the above model results clearly indicate that the seasonal changes are crucial in determining the salinities on the isopycnal surfaces that outcrop in winter. Due to the outcropping, these isopycnal surfaces are blocked from the freshwater source in the northwestern subarctic gyre. Furthermore, the outcropping brings the isopycnal surfaces closer to the turbulent mixed layer, where direct salt input occurs due to the excessive evaporation over the Kuroshio–Oyashio mixed water region.

5. Discussion and conclusions

The existence of a relatively low salinity water mass (the NPIW) that originates in the subarctic North Pacific and penetrates almost throughout the North Pacific subtropical gyre has long been recognized from observations. With the accumulation of observational data, including those from the marginal seas of the North Pacific, our understanding of the NPIW's properties has steadily advanced. Despite this advance, the question of why the spreading of the NPIW in the subtropical North Pacific is preferentially confined to the

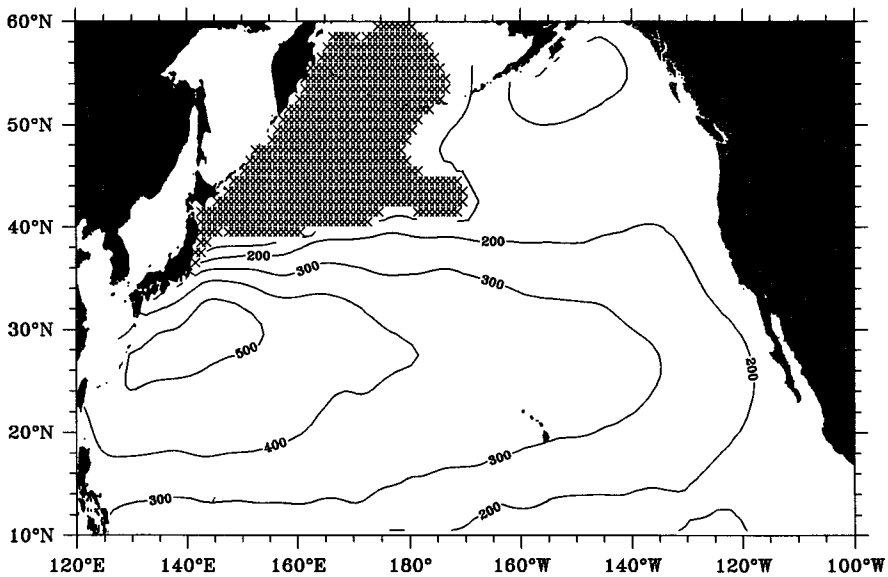

FIG. 10. Depth of the 26.2 σ_θ surface in winter (units are meters). Crosses denote the outcropping area.

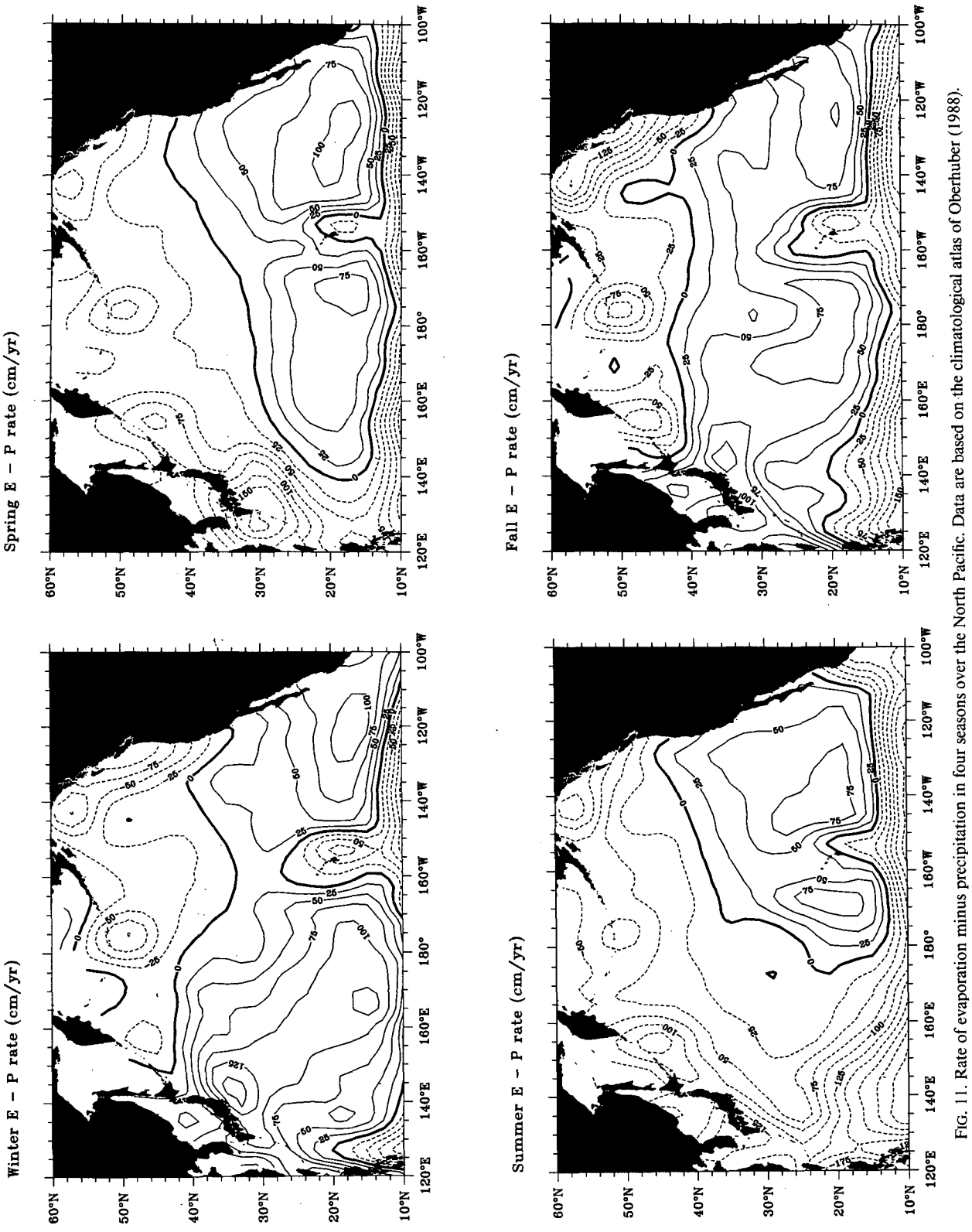

FIG. 11. Rate of evaporation minus precipitation in four seasons over the North Pacific. Data are based on the climatological atlas of Oberhuber (1988).

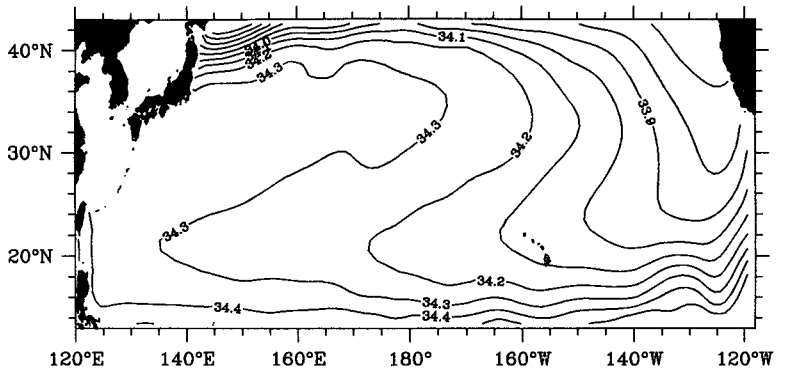

FIG. 12. Same as Fig. 9 except that the observed salinity is specified in the region where the 26.2 σ_θ surface becomes shallower than the seasonally varying mixed layer.

isopycnal surfaces around $\sigma_\theta = 26.8$ remained unsatisfactorily answered.

By combining the Levitus climatological data and an advection–diffusion model, the present study suggested the following mechanism for the confinement of the NPIW around the $\sigma_\theta = 26.8$ surface. For the isopycnal surfaces that do not outcrop in the winter North Pacific ($\sigma_\theta > 26.6$), the salinity distributions are essentially dictated by alongisopycnal advective and diffusive processes. Because the freshwater supply exists in the surface subarctic region, the salinity versus depth characteristic north of the Oyashio Front is such that the salinity increases monotonically with the water depth. As a result of the isopycnal advection and diffusion, this same salinity versus depth characteristic of the subarctic water is carried into the subtropical circulation on these middepth isopycnal surfaces.

For the shallower isopycnal surfaces ($\sigma_\theta < 26.6$), the seasonal outcropping not only interrupts their direct contact with the low-salinity subarctic water but also uplifts the isopycnal surfaces close to the surface mixed layer in the Kuroshio–Oyashio mixed water region. Because the local evaporation exceeds precipitation in fall/winter, the enhanced turbulent mixing in the surface mixed layer helps conduit the surface salt flux onto these outcropping surfaces. The lighter the isopycnal surface is, the greater the conduited salt flux becomes, since the local $E - P$ rate increases monotonically southward (Fig. 11). The result of this seasonal dependency is that the salinity versus depth characteristic for the outcropping isopycnal surfaces in the subtropical region is opposite to that in the subarctic region; namely, the salinity increases as the water depth decreases. Being the lightest density surfaces that undergo no such seasonal change, the isopycnals with $\sigma_\theta = 26.7$–26.9 are unique in the sense that the tongue of the freshest subarctic water can penetrate into the subtropical circulation (see Figs. 2–4). Should the isopycnal surface of $\sigma_\theta = 26.8$ outcrop in the winter North Pacific, the present model suggests that the core of the NPIW would reside on a denser isopycnal surface.

Since the source of freshwater is located north of the Oyashio Front, one question that arises is how the freshwater is transported across the front. By examining the distribution of water properties across the Gulf Stream, Bower et al. (1985) found that the density front of the Gulf Stream imposes a barrier for water masses only in the upper thermocline where the along-isopycnal potential vorticity gradient exists ($\sigma_\theta < 27.1$). Below the 27.1 σ_θ surface where the along-isopycnal potential vorticity is uniform, property fields appeared to be efficiently homogenized by mesoscale exchanges across the Gulf Stream. Across the Oyashio Front, the high-resolution CTD observations (Figs. 2–4) also revealed the transition of the alongisopycnal potential vorticity from an upper layer with strong horizontal gradient to a subsurface layer (below 26.6 σ_θ) where it is mostly uniform. In this subsurface layer, we expect the alongisopycnal diffusion and advection, like across the Gulf Stream, to be efficient. It is thus not coincidence that the shallowest uniform potential vorticity layer corresponds closely to where the spreading of the NPIW occurs.

In the surface layer, the nonuniformity in the potential vorticity implies that the water properties are subject to local atmospheric forcings. In the present study, we emphasized the seasonal outcropping of the density surfaces above $\sigma_\theta = 26.6$ and showed that the positive $E - P$ flux in the winter Kuroshio–Oyashio mixed water region is responsible for the saltier upper layer above the NPIW core. It has long been recognized that a connection exists between the winter conditions at the sea surface and the water mass characters in the permanent thermocline (e.g., Iselin 1939). A physical explanation for this connection has been given by Stommel (1979): the mixed layer density and depth reach their maxima in late winter, and since the mixed layer collapses rapidly in early spring, water subducted into the permanent thermocline is strongly biased toward the late winter values. Stommel's theory seems to explain the model result that even though the isopycnal outcropping occurs locally in space and short

in time, the positive $E - P$ fluxes received by the outcropping layers contribute significantly to the salt content in the ventilated, subtropical North Pacific.

Finally, we note that the advection–diffusion model used in the present study is highly simplified. The along-isopycnal velocities were calculated from the Levitus seasonal/annual climatological data, which may have underestimated the intensity of the Kuroshio and its extension. In estimating the effect of the diapycnal mixing near the outcropping lines, the observed salinity values have been specified diagnostically. To better simulate the salinity patterns in the ventilated upper layer, we clearly need to understand the detailed turbulent mixing processes in the winter mixed layer. Another important point that needs to be addressed in future studies of the NPIW is why 26.8 σ_θ is the least dense isopycnal surface that does not outcrop in the North Pacific. Because of its diagnostic nature, the present model was not designed to address this question. To do so, a more sophisticated ocean model that includes both air–sea interaction processes and the global water mass balance is required.

Acknowledgments. This study was initiated through many discussions with Terrence Joyce, whose advice is gratefully acknowledged. I am also thankful to Fredrick Bingham, Roger Lukas, Julian McCreary, Susan Wijffels, and the reviewers for their critical comments. The hydrographic data used in section 2 were provided by the WOCE Hydrographic Office at the Woods Hole Oceanographic Institution. This study was supported by the Office of Naval Research under Grant N00014-92-J-1656.

REFERENCES

Bingham, F. M., and R. Lukas, 1994: The southward intrusion of North Pacific Intermediate Water along the Mindanao coast. *J. Phys. Oceanogr.*, **24,** 141–154.

Bower, A. S., H. T. Rossby, and J. L. Lillibridge, 1985: The Gulf Stream—Barrier or blender. *J. Phys. Oceanogr.*, **15,** 24–32.

Cochrane, J. D., F. J. Kelly Jr., and C. R. Olling, 1979: Subthermocline countercurrents in the western equatorial Atlantic Ocean. *J. Phys. Oceanogr.*, **9,** 724–738.

Hall, M. M., and N. P. Fofonoff, 1993: Downstream development of the Gulf Stream from 68° to 55°W. *J. Phys. Oceanogr.*, **23,** 225–249.

Hanawa, K., 1987: Interannual variations of the winter-time outcrop area of subtropical mode water in the western North Pacific Ocean. *Atmos. Ocean,* **25,** 358–374.

——, and I. Hoshino, 1988: Temperature structure and mixed layer in the Kuroshio region over the Izu Ridge. *J. Mar. Res.*, **46,** 683–700.

Hasunuma, K., 1978: Formation of the intermediate salinity minimum in the northwestern Pacific Ocean. *Bull. Ocean Res. Inst., University of Tokyo,* **9,** 47 pp.

Hellerman, S., and M. Rosenstein, 1983: Normal monthly wind stress over the World Ocean with error estimates. *J. Phys. Oceanogr.*, **13,** 1093–1304.

Hsiung, J., 1985: Estimates of global oceanic meridional heat transport. *J. Phys. Oceanogr.*, **15,** 1405–1413.

Iselin, C. O. D., 1939: The influence of vertical and lateral turbulence on the characteristics of the waters at mid-depths. *Trans. Amer. Geophys. Union,* **20,** 414–417.

Jenkins, W. J., 1991: Determination of isopycnal diffusivity in the Sargasso Sea. *J. Phys. Oceanogr.*, **21,** 1058–1061.

Joyce, T. M., 1987: Hydrographic sections across the Kuroshio Extension at 165°E and 175°W. *Deep-Sea Res.*, **34,** 1331–1352.

——, and W. J. Schmitz Jr., 1988: Zonal velocity structure and transport in the Kuroshio Extension. *J. Phys. Oceanogr.*, **18,** 1484–1494.

Kawai, H., 1972: Hydrography of the Kuroshio Extension. *Kuroshio—Its Physical Aspects,* H. Stommel and K. Yoshida, Eds., University of Tokyo Press, 235–354.

Levitus, S., 1982: Climatological atlas of the World Ocean. NOAA Prof. Paper No. 13, U.S. Govt. Printing Office, Washington, DC, 173 pp.

Luyten, J. R., J. Pedlosky, and H. Stommel, 1983: The ventilated thermocline. *J. Phys. Oceanogr.*, **13,** 292–309.

Masuzawa, J., 1969: Subtropical mode water. *Deep-Sea Res.*, **16,** 463–472.

——, 1972: Water characteristics of the North Pacific central region. *Kuroshio—Its Physical Aspects,* H. Stommel and K. Yoshida, Eds., University of Tokyo Press, 95–127.

Niiler, P. P., W. J. Schmitz Jr., and D. K. Lee, 1985: Geostrophic volume transport in high eddy-energy areas of the Kuroshio Extension and the Gulf Stream. *J. Phys. Oceanogr.*, **15,** 825–843.

Oberhuber, J. M., 1988: An atlas based on the "COADS" data set: The budgets of heat, buoyancy, and turbulent kinetic energy at the surface of global ocean. Max-Planck-Institute for Meteorology, Report, 15, 199 pp.

Qiu, B., and K. A. Kelly, 1993: Upper ocean heat balance in the Kuroshio Extension region. *J. Phys. Oceanogr.*, **23,** 2027–2041.

Reid, J. L., 1965: Intermediate water of the Pacific Ocean. *Johns Hopkins Oceanographic Studies,* **2,** 58 pp.

Rhines, P. B., and W. R. Young, 1982: A theory of the wind-driven circulation. I. Mid-ocean gyres. *J. Mar. Res.*, **40** (Suppl.), 559–596.

Roemmich, D., and T. McCallister, 1989: Large scale circulation of the North Pacific Ocean. *Progress in Oceanography,* Vol. 22, Pergamon, 171–204.

Stommel, H., 1979: Determination of water mass properties of water pumped down from the Ekman layer to the geostrophic flow below. *Proc. Natl. Acad. Sci. USA,* **76,** 3051–3055.

Sverdrup, H., M. Johnson, and R. Fleming, 1942: *The Oceans.* Prentice-Hall Inc., 1087 pp.

Talley, L. D., 1984: Meridional heat transport in the Pacific Ocean. *J. Phys. Oceanogr.*, **14,** 231–241.

——, 1985: Ventilation of the subtropical North Pacific: The shallow salinity minimum. *J. Phys. Oceanogr.*, **15,** 633–649.

——, 1988: Potential vorticity distribution in the North Pacific. *J. Phys. Oceanogr.*, **18,** 89–106.

——, 1991: An Okhotsk Sea water anomaly: Implications for ventilation in the North Pacific. *Deep-Sea Res.*, **38** (Suppl.), 171–190.

——, 1993: Distribution and formation of North Pacific Intermediate Water. *J. Phys. Oceanogr.*, **23,** 517–537.

Van Scoy, K., D. Olson, and R. Fine, 1991: Ventilation of the North Pacific Intermediate Water: The role of Alaskan Gyre. *J. Geophys. Res.*, **96,** 16 801–16 810.